

## RESEARCH ARTICLE

# Calculation of the Forearm and Hand Three-Dimensional Anthropometry Based on Two-Dimensional Image Feature Extraction: An Approach for Cock-up Splint Design

Mahla Daliri, MD; Mahla Rajabi, MD; Sedigheh Rastaghi, PhD; Mehdi Ataei Azimi, MD; Mona Meybodi, BA; Nafiseh Jirofti, PhD; Mohadeseh Mohadesi, PhD; Afsaneh Jahani, PhD; Ali Moradi, MD, PhD

Research performed at Orthopedics Research Center, Ghaem Hospital, Mashhad University of Medical Sciences (MUMS), Mashhad, Iran

Received: 7 August 2023

Accepted: 15 April 2024

## Abstract

**Objectives:** An alternative to both the time-consuming traditional and the expensive three-dimensional (3D) methods for splint design is to use two-dimensional (2D) images. The present study utilized image processing to achieve an automatic and practical method of anthropometry measurement to design and build a personalized and remote cock-up splint. This method is applicable for patients unable to personally attend clinic appointments.

**Methods:** The defined landmarks of the cock-up splint of 100 adult participants were measured manually. Each individual had a 2D image taken of their upper limb using a customized imaging device. The 2D image portions that corresponded to the manual measurements were then identified, and their sizes were retrieved in pixels using MATLAB software. To find equations between manual 3D measurements and 2D image processing ones, multiple linear regression analysis was performed on landmark variables.

**Results:** We were able to determine equations to estimate manual dimensions based on 2D image data. In the men's group, we could predict the third finger length, forearm circumference at three levels, and the largest forearm circumference. In the women's group, in addition to variables predicted for men, hand circumference at the distal palmar crease and first web levels, as well as arm circumference, could be predicted using the identified equations.

**Conclusion:** Based on the findings, 2D image processing could be an appropriate method for designing personalized cock-up splints.

**Level of evidence:** III

**Keywords:** Customized splint, Forearm landmarks, Image processing, MATLAB

## Introduction

Anthropometry allows for the development of rehabilitative devices and artificial limbs, as well as a casting procedure tailored to individual anatomical features, which can result in standard-fit products.<sup>1,2</sup> Conventional casting and splinting methods are associated with problems for both the patient and the person preparing the cast. If the splint is too tight or too

loose, it may need to be released or adjusted, which requires the casting process to be repeated.<sup>3</sup> In addition, problems such as heavy weight, inability to bathe, inability to pass air, increased risk of skin diseases (such as infection, dermatitis, as well as pressure sores), and heat damage can threaten the patient,<sup>4-6</sup> especially when casting is performed by an inexperienced individual.<sup>7</sup>

### Corresponding Author:

- 1- Afsaneh Jahani, Orthopedic Research Center, Mashhad University of Medical Science, Mashhad, Iran/ Department of Biomedical Engineering, Faculty of New Sciences and Technologies, Semnan University, Semnan, Iran. Email: afsane\_j70@yahoo.com
- 2- Ali Moradi, Orthopedics Research Center, Ghaem Hospital, Mashhad University of Medical Sciences, Mashhad, Iran. Email: Moradial@MUMS.ac.ir



THE ONLINE VERSION OF THIS ARTICLE  
ABJS.MUMS.AC.IR



Although prefabricated splints are available, they are not generally customized, and custom-made ones take time and may require trimming.<sup>8</sup> This becomes particularly problematic in cases where the patient needs serial casting, necessitating more standard and easier methods of casting or splinting.<sup>9</sup> Therefore, it is essential to have a system to measure human body metrics for creating fitting splints and casts. While the existing three-dimensional (3D) measurement approaches are a reasonable solution, they are inconvenient due to high expenses and the necessity of an in-person clinical visit. According to previous studies, using two-dimensional images (2D) for anthropometric measurements can be a good alternative to both the time-consuming traditional and the expensive 3D methods,<sup>1,10</sup> as it has the potential to act as a practical measurement tool independent of the operator. Furthermore, the primary benefit of this approach lies in its facilitation of telemedicine and telerehabilitation for creating braces remotely, which reduces time and travel costs.<sup>11</sup> Additionally, in situations such as the COVID-19 pandemic, telerehabilitation becomes even more significant<sup>12</sup> to facilitate telemedicine by providing a direct uplink of the 3D model and data to be reviewed by a remote medical professional.

The present study was conducted to propose an automatic and practical method of anthropometry measurement for designing and developing a customized cock-up splint using image processing. The determined landmarks of the cock-up splint, which are detectable by MATLAB, are analyzed to obtain equations that can be used to calculate the actual 3D size of the limb circumference from 2D image parameters, allowing for the design and construction of cock-up limb thermoplastic splints for that specific limb. Therefore, this study tries to identify the equation between the manually measured 3D dimensions of the limb and MATLAB 3D dimensions extracted from 2D image parameters for designing a cock-up splint.

## Materials and Methods

### Setting

This study was performed between 2018 and 2021 in the

interdisciplinary setting of Mashhad University of Medical Sciences (MUMS) and Engineering Faculty of Ferdowsi University, Mashhad, Iran. The team consisted of electronics experts, mechanics experts, computer engineers, orthopedic specialists, and a statistics expert.

### Participants' Descriptive Data

Overall, 100 adult participants (52 men and 48 women) with a mean age of 40.76 (range: 18 to 82) who visited the orthopedics clinic of our tertiary hospital were randomly recruited for this study [Table 1]. The inclusion criteria were being over 18 years old and having at least one healthy upper limb. On the other hand, the exclusion criteria were dissatisfaction with participating in the study or having inseparable jewelry, long nails, tattooing, nevus, bulging, fracture, deformity, or any disease affecting limb anthropometry, such as lymphedema.

### Research Design

The idea of creating personalized upper extremity splints using 2D images was conceived in 2016. After a thorough review of relevant literature, we piloted this concept with 30 participants in a previous study. We manually measured both 2D and 3D image indices to develop formulas that allowed us to derive 3D measurements from simple 2D images. Subsequently, utilizing the formulas derived from our pilot study, we designed an imaging system device capable of capturing 2D images of the upper limb. These images serve as the basis for designing a 3D cock-up splint pattern on a thermoplastic shield using the provided dimensional data (Patent No. A61F 5/058 (2018.01)). Finally, the final version of the device was developed. In the present study, the critical parts of a cock-up splint,<sup>8</sup> which were also detectable by MATLAB software, were chosen and measured manually for the participants' upper limbs. The selected anatomical landmarks are illustrated in [Figure 1C and Table 2]. MATLAB software was used to process the 2D images and extract the approximate 3D measures.

Table 1. Demographic characteristics of the participants (n=100)

Gender	Number	Age (year)			BMI		
		Min	Max	Mean ( $\pm$ SD)	Min	Max	Mean ( $\pm$ SD)
Female	48	18	81	44.5 ( $\pm$ 14.57)	18.1	42.32	29.35 ( $\pm$ 6.1)
Male	52	18	82	37.22 ( $\pm$ 15.91)	16.4	40.35	26.26 ( $\pm$ 5.18)
<b>Total</b>	<b>100</b>	<b>18</b>	<b>82</b>	<b>40.76 (<math>\pm</math>15.63)</b>	<b>16.4</b>	<b>42.32</b>	<b>27.74 (<math>\pm</math>5.8)</b>

Table 2. Definition of variables based on anatomical landmarks

Variable	Definition
A	The third finger length: From the proximal crease at the base of the finger to the fingertip
B	Hand circumference: At the distal palmar crease level, from the radial to the ulnar side
G	Hand circumference: At the first web level, in parallel with variable B
H	A line from the first web to the styloid process
J	Wrist circumference: The radius styloid process level, in line with the wrist distal crease

Table 2. Continued	
K	Forearm circumference: From the wrist distal crease to the proximal at three distance levels: the third finger length (K1), twice of the third finger length (K2), twice and a half of the third finger length (K3)
L	The forearm's largest diameter detected by sight and moving the tape
N <sub>e</sub>	Distance from the middle of the L to the middle of the J while the forearm is extended
N <sub>r</sub>	Distance from the middle of the L to the middle of the J while the forearm is flexed
I	The first finger width at the MCP joint level
M	Arm diameter: At the distance equal to the hand third finger, proximal to the elbow
O	Distance from the middle of the distal crease of the elbow to M
P	The third finger length: From the MCP joint to the fingertip
R	The fifth finger length, from the MCP joint to the fingertip, with the finger extended and abducted
Q	Dorsum hand length: From the MCP joint to the wrist (at the line crossing the ulnar and radial styloid processes) at three positions: neutral (Q1), wrist thirty-degree extension (Q2), and wrist thirty-degree flexion (Q3)

## Tools

### 1. Imaging Device

The cube-shaped device, with a size of 110×40×110, consists of two cameras, a glass limb holder [Figure 1A], wheels for easy transportation, and blue light LEDs. Yellow light is also shining from the floor. One camera was mounted on the device's floor, while the other was mounted on its lateral wall. The features of the full-HD color digital Canon EOS 1200D+1855 III cameras [Figure 1B] are as follows: 1) size: 130×100×78 mm, 2) weight: 480 g, 3) body material: composite, 4) F-stop: f/16, 5) exposure time: 1/20 second, 6) ISO 400, 7) focal length: 20 mm, and 8) photo resolution: 5194×3456 pixels.

Blue light was employed in the imaging apparatus to achieve the greatest contrast between the limb outlines and

the background glass because the spectrum of blue light in different skin hues is narrower than the range of green and red light. The item designation was in such a way that the ambient light and the light reflection inside the device were decreased to zero. Because the glass on which the limb was lying could cause light parasites in the illumination, the lowest possible thickness was adopted for it. Considering the possibility of participants' insufficient cooperation and the glass break, it was not possible to reduce the glass thickness more or omit it. Image calibration was required to modify the anatomical disparities between the limbs. It was accomplished by employing the metal clamp of the device, which can be seen in all images. The confounding variable, limb hair, was modified by regulating the blue light concentration.

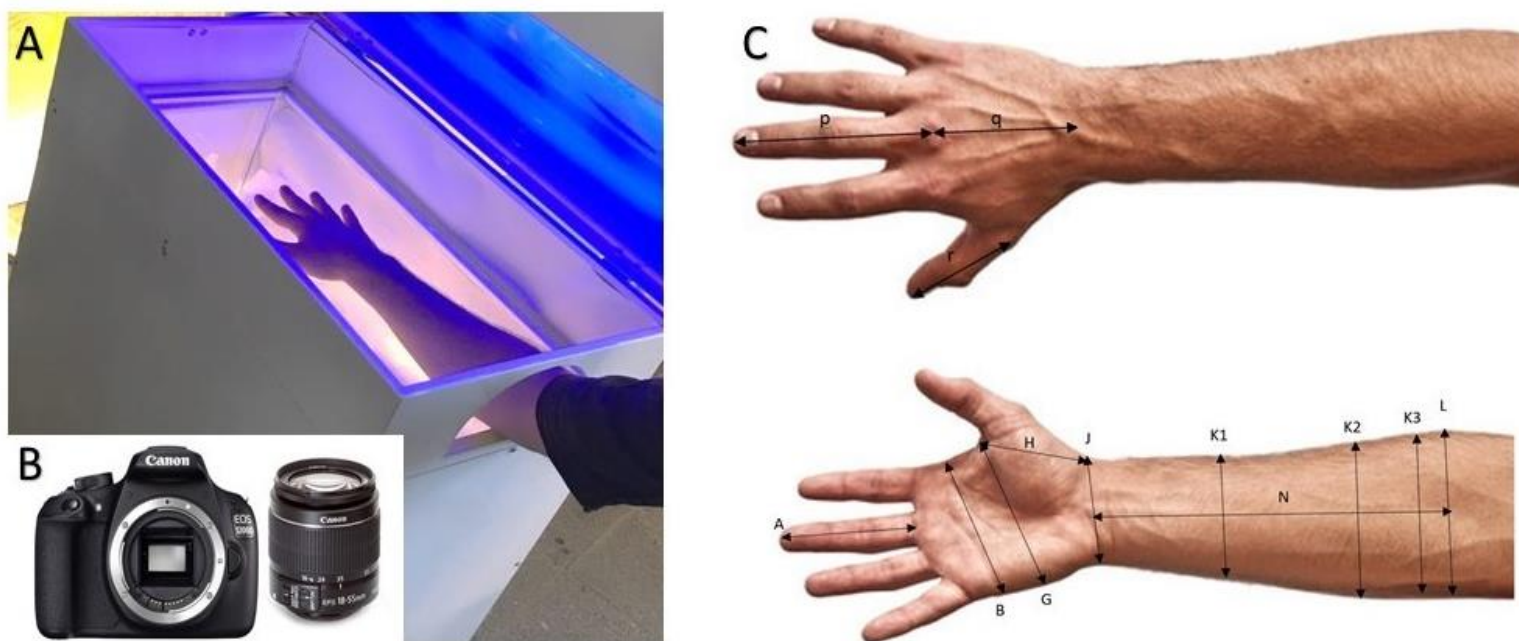


Figure 1. Imaging device (A), ESO 1200D Canon camera used in the imaging device (B), and measured variables due to anatomical landmarks (C)

## 2. Paper Tapes and Caliper

Thin, identical paper tapes were designed in a millimeter unit (length: 50 cm, width: 0.5 cm) to manually measure all the landmarks mentioned. The material of the measuring tool, as well as its flexibility, was critical to us. Since the precision of plastic measuring meters gradually diminishes after multiple measurements, paper tapes with millimeter accuracy were created in our study. To reduce manual measuring errors, one person did the measurements while another served as the controller. A caliper was used to measure the line from the first web to the styloid process (variable H).

## 3. MATLAB Software

Image processing was conducted by MATLAB software (version R2019a). The image 2D parameters were measured, and the 3D dimensions were reported based on the defined algorithms. The image thresholding was applied to extract the limb image out of the background. The limb borders were identified using the Hough method,<sup>13,14</sup> and morphologic algorithms were utilized to enhance the border quality, allowing for more precise processing. The difference between right and left limbs was considered in the MATLAB software program.

### Manual Measurement Method

Measurements were conducted at the palmar side of the limb with the wrist positioned with a slight extension angle, the forearm in supination (except for variables Q, P, I, and R, which were measured at the dorsal side in forearm

pronation), the wrist in the neutral position, the fingers fully abducted, and the hand resting on the floor surface of the imaging device [Figure 1A]. The circumference and the length of the selected parameters were measured manually and recorded by a trained researcher. The thenar area was measured with a caliper, while the other landmarks were measured with the created paper tapes.

### 2D Measurement Method

In the next step, a 2D image of the palmar side of each participant's upper limb was taken, from elbow to fingertips [Figure 2A]. The limb pattern was extracted by MATLAB software, removing the blue background [Figure 2B]. The parts corresponding to the manual components were then identified using MATLAB software, and their size was extracted in pixels. Anatomic landmarks, such as hand palmar creases, fingertips, and the webs, were used in image processing. To extract the limb 3D measurements out of a 2D image, MATLAB detected the wrist as the narrowest part of the forearm. The forearm borders were then figured out as lines parallel to the third finger. After that, the limb was divided into proximal (forearm) and distal (hand) parts, and thus the wrist was detected as the border between the two parts [Figure 2C]. To measure the B variable, the palm was imagined as a circle with a diameter from the palm center to the wrist [Figure 2D]. K1, K2, and K3 locations were excreted on a line along the third finger, and the widths were measured in pixels. The L parameter was also detected as the largest width of the forearm.

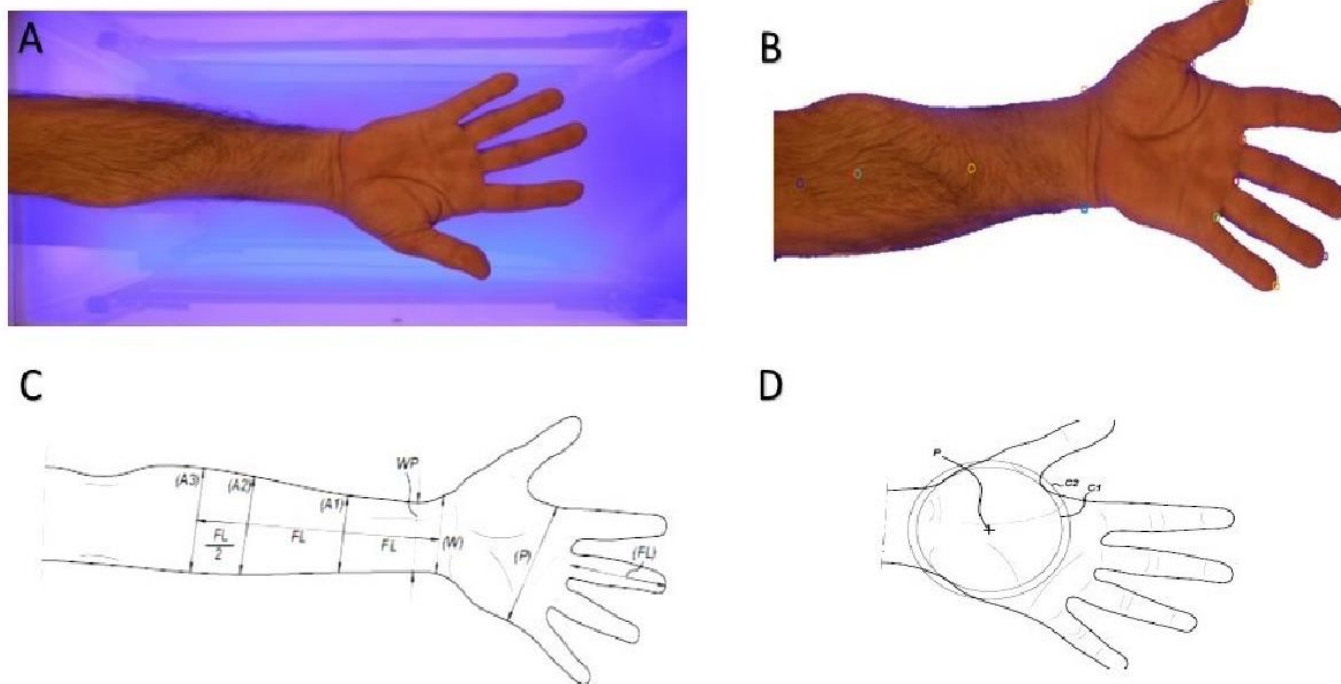


Figure 2. Two-dimensional picture of the limb taken by the ESO 1200D camera (A), extracted limb pattern after removing the blue background and detection of the measurement points by MATLAB software (B), detection and excretion of image parameters by MATLAB software (C), and excretion of parameter B by MATLAB software (D)

**Statistical Analysis**

Statistical analysis was performed using SPSS software (version 16). Considering the lowest correlation between the forearm diameter and circumference,<sup>15</sup> as well as the sample size in similar studies, the sample size was estimated at 50 in this study. It was, however, doubled to 100 when gender was taken into account.

First, the normality of the data distribution was checked by the one-sample Kolmogorov-Smirnov test. Due to a significant difference in limb circumference between the two genders (as determined by an independent samples t-test) and the accuracy needed in millimeters, the data were divided into two groups: men and women. Using scatter plot charts, the linear correlation between all the dependent (manual measurements) and independent (2D image processing data) variables was checked. The scattering of variables was also assessed, and the best correlations were selected. Linear correlation was evaluated between the 2D image data and the manual measurement data using Pearson's correlation coefficient. To find equations between manual and 2D image measurements, first, variables with the strongest correlation were included in multiple linear regression analysis. After that, according to the relationship between any of the independent and dependent variables,

independent variables with the lowest correlation were omitted one by one. This continued until the R-value was maintained at its best. Finally, equations with the highest R-value and the fewest independent variables were extracted, and the results of the equation calculations were compared to the manual data. All P-values below than 0.05 were evaluated statistically significant. The analysis was conducted using SPSS software, version 19.

**Results****Regression between Manual Data and Image Variables**

Using linear regression analysis with the backward method, the following final results were obtained in the men's group [Table 3]. Image variable A was a predictor of manual variable A at the hand middle finger length ( $P < 0.001$  and  $R^2 = 0.913$ ). Image variables B ( $P = 0.004$ ) and K1 ( $P < 0.001$ ) were predictors of manual variable K1 ( $R^2 = 0.706$ ). Image variables K1 ( $P < 0.001$ ), K3 ( $P = 0.025$ ), K2 ( $P = 0.005$ ), and A ( $P = 0.035$ ) were predictors of manual variable K2 ( $R^2 = 0.737$ ). Image variables K1 ( $P < 0.001$ ), K2 ( $P = 0.063$ ), and A ( $P = 0.016$ ) were predictors of manual variable K3 ( $R^2 = 0.646$ ). Image variables K1 ( $P < 0.001$ ) and A ( $P = 0.007$ ) were predictors of manual variable L ( $R^2 = 0.646$ ).

**Table 3. Linear regression analysis between image variables, manual variables, and extracted equations in the men's group**

Dependent variable (Manual)	Independent variable (Image)	Unstandardized coefficients		t	P-value	Model determination coefficient	Regression equation by image data (mm)																																																																															
		B	Std. Error																																																																																			
A	(Constant)	7.232	3.183	2.272	0.027	R Square=0.913	7.232+0.033 A																																																																															
	mmpixA	0.033	0.001	22.885	0.000			K1	(Constant)	105.982	17.188	6.166	0.000	R Square=0.706	105.982+0.091 K1-0.022 B	mmpixK1	0.091	0.009	10.660	0.000	mmpixB	-0.022	0.008	-2.990	0.004	K2	(Constant)	129.615	26.101	4.966	0.000	R Square=0.737	129.615+0.097 K1+0.045 K2- 0.033 K3-0.025 A	mmpixK1	0.097	0.016	6.111	0.000	mmpixK2	0.045	0.016	2.919	0.005	mmpixK3	-0.033	0.014	-2.319	0.025	K3	(Constant)	165.928	29.258	5.671	0.000	R Square=0.646	165.928+0.087 K1+0.016 K2- 0.032 A	mmpixK1	0.087	0.018	4.849	0.000	mmpixK2	0.016	0.009	1.905	0.063	mmpixA	-0.032	0.013	-2.490	0.016	L	(Constant)	169.702	28.606	5.932	0.000	R Square=0.646	169.702+.114 K1-0.036 A	mmpixK1	0.114	0.012	9.465	0.000	mmpixA	-0.036
K1	(Constant)	105.982	17.188	6.166	0.000	R Square=0.706	105.982+0.091 K1-0.022 B																																																																															
	mmpixK1	0.091	0.009	10.660	0.000																																																																																	
	mmpixB	-0.022	0.008	-2.990	0.004																																																																																	
K2	(Constant)	129.615	26.101	4.966	0.000	R Square=0.737	129.615+0.097 K1+0.045 K2- 0.033 K3-0.025 A																																																																															
	mmpixK1	0.097	0.016	6.111	0.000																																																																																	
	mmpixK2	0.045	0.016	2.919	0.005																																																																																	
	mmpixK3	-0.033	0.014	-2.319	0.025																																																																																	
K3	(Constant)	165.928	29.258	5.671	0.000	R Square=0.646	165.928+0.087 K1+0.016 K2- 0.032 A																																																																															
	mmpixK1	0.087	0.018	4.849	0.000																																																																																	
	mmpixK2	0.016	0.009	1.905	0.063																																																																																	
	mmpixA	-0.032	0.013	-2.490	0.016																																																																																	
L	(Constant)	169.702	28.606	5.932	0.000	R Square=0.646	169.702+.114 K1-0.036 A																																																																															
	mmpixK1	0.114	0.012	9.465	0.000																																																																																	
	mmpixA	-0.036	0.013	-2.827	0.007																																																																																	

Based on the linear regression analysis, the following results were obtained in the women's group [Table 4]. Image variable A was a predictor of manual variable A ( $P < 0.001$  and  $R^2 = 0.915$ ). Image variables K2 ( $P < 0.001$ ) and B ( $P < 0.001$ ) were predictors of manual variable B ( $R^2 = 0.626$ ). Image

variables K2 ( $P = 0.001$ ), K3 ( $P = 0.011$ ), A ( $P = 0.039$ ), and J ( $P < 0.001$ ) were predictors of manual variable K1 ( $R^2 = 0.810$ ). Image variables K2 ( $P < 0.001$ ), K3 ( $P = 0.002$ ), and J ( $P = 0.022$ ) were predictors of manual variable K2 ( $R^2 = 0.841$ ). Image variables K2 ( $P = 0.004$ ), K3 ( $P < 0.001$ ),

and J (P=0.005) were predictors of manual variable K3 (R2=0.810). Image variables K2 (P<0.001) and K3 (P=0.002) were predictors of manual variable L (R2=0.764). Image

variables K2 (P<0.001), L (P=0.001), and J (P=0.020) were predictors of manual variable M (R2=0.689).

**Table 4. Linear regression analysis between image variables, manual variables, and extracted equations in the women's group**

Dependent variable (Manual Variable)	Independent variable (Image Variable)	Unstandardized coefficients		t	P-value	Model determination coefficient	Regression equation By image data (mm)																																																																																																																																																														
		B	Std. Error																																																																																																																																																																		
A	(Constant)	-0.136	3.377	-0.040	0.968	R Square=0.915	-0.136+0.037 A																																																																																																																																																														
	mmpix A	0.037	0.002	22.212	0.000			B	(Constant)	71.856	16.597	4.329	0.000	R Square=0.626	71.856+0.021 K2+0.041 B	mmpix K2	0.021	0.005	4.415	0.000	mmpix B	0.041	0.008	4.836	0.000	G	(Constant)	66.192	20.113	3.291	0.002	R Square=0.733	66.192+0.026 K2-0.019 A+0.063 B	mmpix K2	0.026	0.005	5.229	0.000	mmpix A	-0.019	0.010	-1.968	0.055	mmpix B	0.063	0.010	6.328	0.000	K1	(Constant)	21.201	31.599	0.671	0.506	R Square=0.810	21.201+0.074 J+0.045 K2+0.025 K3-0.033 A	mmpix J	0.074	0.016	4.550	0.000	mmpix K2	0.045	0.013	3.556	0.001	mmpix K3	0.025	0.009	2.644	0.011	mmpix A	-0.033	0.015	-2.132	0.039	K2	(Constant)	31.099	18.978	1.639	0.108	R Square=0.841	31.099+0.035 J+0.061 K2+0.030 K3	mmpix J	0.035	0.015	2.366	0.022	mmpix K2	0.061	0.012	5.053	0.000	mmpix K3	0.030	0.009	3.374	0.002	K3	(Constant)	91.127	32.603	2.795	0.008	R Square=0.810	91.127+0.049 J+0.040 K2+0.040 K3-0.028 A	mmpix J	0.049	0.017	2.941	0.005	mmpix K2	0.040	0.013	3.076	0.004	mmpix K3	0.040	0.010	4.098	0.000	mmpix A	-0.028	0.016	-1.801	0.079	L	(Constant)	98.091	13.461	7.287	0.000	R Square=0.764	98.091+0.058 K2+0.033 K3	mmpix K2	0.058	0.013	4.408	0.000	mmpix K3	0.033	0.010	3.344	0.002	M	(Constant)	116.334	38.119	3.052	0.004	R Square=0.689	116.334-0.071 J+0.090 K2+0.059 L	mmpix J	-0.071	0.029	-2.413	0.020	mmpix K2	0.090	0.023	3.871	0.000	mmpix L	0.059
B	(Constant)	71.856	16.597	4.329	0.000	R Square=0.626	71.856+0.021 K2+0.041 B																																																																																																																																																														
	mmpix K2	0.021	0.005	4.415	0.000																																																																																																																																																																
	mmpix B	0.041	0.008	4.836	0.000																																																																																																																																																																
G	(Constant)	66.192	20.113	3.291	0.002	R Square=0.733	66.192+0.026 K2-0.019 A+0.063 B																																																																																																																																																														
	mmpix K2	0.026	0.005	5.229	0.000																																																																																																																																																																
	mmpix A	-0.019	0.010	-1.968	0.055																																																																																																																																																																
	mmpix B	0.063	0.010	6.328	0.000																																																																																																																																																																
K1	(Constant)	21.201	31.599	0.671	0.506	R Square=0.810	21.201+0.074 J+0.045 K2+0.025 K3-0.033 A																																																																																																																																																														
	mmpix J	0.074	0.016	4.550	0.000																																																																																																																																																																
	mmpix K2	0.045	0.013	3.556	0.001																																																																																																																																																																
	mmpix K3	0.025	0.009	2.644	0.011																																																																																																																																																																
	mmpix A	-0.033	0.015	-2.132	0.039																																																																																																																																																																
K2	(Constant)	31.099	18.978	1.639	0.108	R Square=0.841	31.099+0.035 J+0.061 K2+0.030 K3																																																																																																																																																														
	mmpix J	0.035	0.015	2.366	0.022																																																																																																																																																																
	mmpix K2	0.061	0.012	5.053	0.000																																																																																																																																																																
	mmpix K3	0.030	0.009	3.374	0.002																																																																																																																																																																
K3	(Constant)	91.127	32.603	2.795	0.008	R Square=0.810	91.127+0.049 J+0.040 K2+0.040 K3-0.028 A																																																																																																																																																														
	mmpix J	0.049	0.017	2.941	0.005																																																																																																																																																																
	mmpix K2	0.040	0.013	3.076	0.004																																																																																																																																																																
	mmpix K3	0.040	0.010	4.098	0.000																																																																																																																																																																
	mmpix A	-0.028	0.016	-1.801	0.079																																																																																																																																																																
L	(Constant)	98.091	13.461	7.287	0.000	R Square=0.764	98.091+0.058 K2+0.033 K3																																																																																																																																																														
	mmpix K2	0.058	0.013	4.408	0.000																																																																																																																																																																
	mmpix K3	0.033	0.010	3.344	0.002																																																																																																																																																																
M	(Constant)	116.334	38.119	3.052	0.004	R Square=0.689	116.334-0.071 J+0.090 K2+0.059 L																																																																																																																																																														
	mmpix J	-0.071	0.029	-2.413	0.020																																																																																																																																																																
	mmpix K2	0.090	0.023	3.871	0.000																																																																																																																																																																
	mmpix L	0.059	0.017	3.499	0.001																																																																																																																																																																

### Mean Error

The difference between predicted and observed 3D measurements was calculated [Table 5]. Considering the normal distribution of variables, all calculated 3D parameters using the obtained formula should be considered with a  $\pm 1$  mm standard deviation.

### Discussion

The primary goal of this study was to extract the 3D size of

the forearm from its 2D image in the areas relevant to a cock-up splint and use it for developing a custom splint. We could find equations, both for men and women, to extract the manual dimensions out of the 2D image data.

### Main Findings

The manual measurement of the forearm circumference (K1) could be predicted by hand (B) and forearm circumference (K1) measured by MATLAB 2D image

processing in the men's group. At twice the third finger length (K2) level, the forearm circumference was correlated with its circumference at all three levels (K1, K2, and K3), as well as the third finger length (A). In addition, the forearm's largest diameter (L) could be predicted by K1 and A. In the women's group, the third finger length (A) and wrist circumference (J) variables measured by MATLAB were

correlated with the forearm circumference (K1). The forearm's largest diameter (L) could be predicted by its circumference (K1 and K2), as measured by MATLAB. The arm diameter (M) could be predicted by the wrist circumference, the maximum forearm circumference, and the forearm circumference at the K2 level.

Table 5. Error descriptive data (mm)

Variable	Standard residual (mean±SD)	
	Men	Women
A	0.00±0.990	0.00±0.989
B	.....	0.00±0.978
G	.....	0.00±0.968
K1	0.00±0.980	0.00±0.957
K2	0.00±0.960	0.00±0.968
K3	0.00±0.970	0.00±0.957
L	0.00±0.980	0.00±0.978
M	.....	0.00±0.968

Data were more scattered in the women's group than in the men's group. We could hypothesize that in addition to gender, job type and activity level are important factors because they influence muscle mass. This finding could imply that as the muscle/fat ratio in a limb increases, the amount of error declines. Another supposition is that the amount of limb fat may influence manual measurements. It also emphasizes the importance of limb pressure on the glass while taking the image. As a result, some adjustments to measuring tools and the design of the imaging apparatus should be considered. Repeating the study with more participants and dividing them into different age groups can help to acquire more accurate results. The error standard deviations can be influenced by multiple factors, such as measurement errors, software errors, image quality, age, race, and the level of activity.

The findings of the current study are consistent with those of Hung, titled "Anthropometric measurements from photographic images computing systems".<sup>16,17</sup> In this study, a Canon color camera was used to evaluate 10 measurements of 20 young men in three different views. The repeatability and accuracy of anthropometric measurements by image-based systems are very close to manual ones performed by skilled people, according to Meunier et al. (2000).<sup>10</sup> The present study shows that the amount of correlation between manual and image measurements depends not only on the skilled operator but also on the accuracy of the image processing method and the body part being measured. Lin et al. (2010) extracted the human body shape out of 2D images taken from a five-meter distance of each participant using a silhouette detection method.<sup>6</sup> However, we could extract more details out of images as we used MATLAB software and took them from a closer distance. In a similar study, Hung et al. used black cloth as the background, which did not make enough contrast with color

clothing, while we used blue light as the background, which makes enough contrast for image processing even for dark skin. Joao W.M et al. tried to predict body measures from 2D images using convolutional neural networks in 2020. Similar to our methodology, they first calculated the diameter of some parts of the body out of a 2D image. After that, they extracted the circumferences, considering each part as a geometric figure. In this study, however, we used the highest correlations between the image and manual data to extract equations and find the circumference.

The inclusion of more limb parameters may lead to more robust relationships between the image data and the manual ones. Increasing the number of participants and considering other effective factors, such as BMI, muscle/fat ratio, race, and age, can result in more accuracy. Similar studies could be conducted for other parts of the body or even for upgrading other industries, such as the production of varicose socks. The findings of this study can be used to replace the existing methods of measuring limb circumference with a mechanized method that leads to more accurate, low-cost, and common diagnostic and treatment criteria. This method allows for the accurate comparison of the circumference of different parts of the limb while reducing the measurement time, especially since it allows for the electronic storage of information about each patient.

### Limitations

This study had a few limitations. First, the small sample size did not allow us to classify the analyses based on age groups. Furthermore, the glass on which the limb was rested could generate light parasites in illumination, so the lowest possible thickness was selected for it. Considering the participants' insufficient cooperation, it was impossible to reduce the glass thickness more or omit it. The pressure of the limb on the glass was an unavoidable issue that could

impact both the image data and manual measurements. In addition, image detection for the longitudinal arch of a hand was not considered for the cock-up splint design. Finally, we suggest future studies determine intra-observer reliability by calculating intraclass correlation coefficients and improve the precision of image processing using AI-based techniques.

### Conclusion

This study set out to extract the 3D size of the forearm out of its 2D image to design an individualized cock-up splint. Based on the results, we could find equations, both for men and women, to extract the manual data out of the image data.

### Acknowledgement

We would like to thank Shahryar Hashemi for preparing the manuscript for submission.

### Authors' Contribution:

Mahla Daliri: Investigation, manuscript writing, and proofreading

Mahla Rajabi: Investigation, manuscript writing, and proofreading

Sedigheh Rastaghi: Statistical analysis

Mehdi Ataei: Investigation and manuscript writing

Mona Meybodi: Investigation and manuscript writing

Nafiseh Jirofti: Investigation and proofreading

Mohadeseh Mohadesi: Investigation and manuscript writing

Afsaneh Jahani: Investigation and proofreading

Ali Moradi: Conceptualization, supervision, methodology, and proofer

**Declaration of Conflict of Interest:** The authors do not have any potential conflicts of interest regarding this manuscript.

**Declaration of Funding:** This study was supported as a research project funded by the Research Council of Mashhad University of Medical Sciences, Mashhad, Iran (research project number: 950493).

**Declaration of Ethical Approval for Study:** The study was approved by the Research Ethics Committee of Mashhad University of Medical Sciences, Mashhad, Iran (approval number: IR.MUMS.fm.REC. 1395.575) (<https://ethics.research.ac.ir/>) and was conducted in accordance with the ethical standards in the 1964 Declaration of Helsinki.

**Declaration of Informed Consent:** All participants were informed of the experiment and were asked to fill out a voluntary consent form. They were also informed that not participating in the study would not affect their treatment process.

Mahla Daliri MD <sup>1\*</sup>

Mahla Rajabi MD <sup>1\*</sup>

Sedigheh Rastaghi PhD <sup>2</sup>

Mehdi Ataei MD <sup>1</sup>

Mona Meybodi BA <sup>1</sup>

Nafiseh Jirofti PhD <sup>1,3</sup>

Mohadeseh Mohadesi PhD <sup>1,3,4</sup>

Afsaneh Jahani PhD <sup>1,3,5</sup>

Ali Moradi MD, PhD <sup>1</sup>

1 Orthopedics Research Center, Department of Orthopedic Surgery, Mashhad University of Medical Sciences, Mashhad, Iran

2 Department of Biostatistics, School of Public Health, Mashhad University of Medical Sciences, Mashhad, Iran

3 Bone and Joint Research Laboratory, Ghaem Hospital, Mashhad University of Medical Science, Mashhad, Iran

4 Department of Pharmaceutics, School of Pharmacy, Mashhad University of Medical Science, Mashhad, Iran

5 Faculty of New Sciences and Technologies, Department of Biomedical Engineering, Semnan University, Semnan, Iran

\*\*First Authors: These authors contributed equally

### References

- Shah C, Shah J, Shaikh M, Sandhu H, Natu P. Anthropometric Measurement Technology Using 2D Images. In Proceedings of Second International Conference on Sustainable Expert Systems: ICSES 2021- 2022 (pp. 127-142). Singapore: Springer Nature Singapore.
- Mojaverrostami S, Najibi A, Mokhtari T, Malekzadeh M, Hassanzadeh G. The Importance and Application of Anthropometry in Medical Sciences and Related Industries: A Narrative Review. Journal of Rafsanjan University of Medical Sciences. 2019; 18(6):606-589.
- Popescu D, Zapciu A, Tarba C, Laptoiu D. Fast production of customized three-dimensional-printed hand splints. Rapid Prototyping Journal. 2020; 26(1):134-144. doi:10.1108/RPJ-01-2019-0009.
- Blaya F, Pedro PS, Silva JL, D'Amato R, Heras ES, Juanes JA. Design of an Orthopedic Product by Using Additive Manufacturing Technology: The Arm Splint. J Med Syst. 2018; 42(3):54. doi: 10.1007/s10916-018-0909-6.
- Boyd AS, Benjamin HJ, Asplund CA. Principles of casting and splinting. Am FAM Physician. 2009; 79(1):16-22.
- Lin Y-L, Wang M-JJ. Automated body feature extraction from 2D images. Expert Systems with Applications. 2011; 38(3):2585-91.
- Halanski M, Noonan KJ. Cast and splint immobilization: complications. J Am Acad Orthop Surg. 2008;16(1):30-40. doi: 10.5435/00124635-200801000-00005.
- Boyd AS, Benjamin HJ, Asplund CA. Splints and casts: indications and methods. Am FAM Physician. 2009; 80(5):491-9.
- Thorndike A, Murphy EF, Staros A. Engineering Applied to Orthopedic Bracing. Orthop and Prosth Appl J. 1956; 10(4):55-71.
- Meunier P, Yin S. Performance of a 2D image-based



- anthropometric measurement and clothing sizing system. *Appl Ergon.* 2000; 31(5):445-51. doi: 10.1016/s0003-6870(00)00023-5.
11. Rivlin M, Sedigh A, Kachooei AR, et al. Apparatus for anatomic three dimensional scanning and automated three dimensional cast and splint design. United States patent application US 17/914,948. 2023.
  12. Sedigh A, Kachooei AR, Vaccaro AR, Rivlin M. Contactless remote 3D splinting during COVID-19: report of two patients. *J Hand Surg Asian Pac Vol.* 2022;27(2):398-402. doi: 10.1142/S2424835522720171.
  13. Wang H, Boyd JP, Akmaev RA. On computation of Hough functions. *Geoscientific Model Development.* 2016; 9(4):1477-148.
  14. Abdi R, Shahpari O, Bagheri F, Zargarbashi R. A Method of Time Prediction in Epiphysiodesis for Limb Length Discrepancy Based On Multiplier. *Arch Bone Jt Surg.* 2023;11.765:(12) doi:<https://doi.org/10.22038/abjs.2023.67521.3205>
  15. Holzbaur KR, Murray WM, Gold GE, Delp SL. Upper limb muscle volumes in adult subjects. *J Biomech.* 2007; 40(4):742-9. doi: 10.1016/j.jbiomech.2006.11.011.
  16. Hung PC-Y, Witana CP, Goonetilleke RS. Anthropometric measurements from photographic images. *Computing Systems.* 2004; 29(764-769):3.
  17. Farzam R, Deilami M, Jalili S. Comparison of Anesthesia Results between Wide Awake Local Anesthesia no Tourniquet (WALANT) and Forearm Tourniquet Bier Block in Hand Surgeries: A Randomized Clinical Trial. *Arch Bone Jt Surg.* 2021;9(1):116 doi:<https://doi.org/10.22038/abjs.2020.49526.2487>